# Acoustic buffeting by infrasound in a low vibration facility

# Acoustic buffeting by infrasound in a low vibration facility

B. P. MacLeod,[1] J. E. Hoffman,[2] S. A. Burke,[1,2] and D. A. Bonn[2,a)]
[1]*Department of Chemistry, University of British Columbia, Vancouver, British Columbia V6T 1Z1, Canada*
[2]*Department of Physics and Astronomy, University of British Columbia, Vancouver, British Columbia V6T 1Z1, Canada*

(Received 31 May 2016; accepted 13 August 2016; published online 9 September 2016)

Measurement instruments and fabrication tools with spatial resolution on the atomic scale require facilities that mitigate the impact of vibration sources in the environment. One approach to protection from vibration in a building's foundation is to place the instrument on a massive inertia block, supported on pneumatic isolators. This opens the questions of whether or not a massive floating block is susceptible to acoustic forces, and how to mitigate the effects of any such acoustic buffeting. Here this is investigated with quantitative measurements of vibrations and sound pressure, together with finite element modeling. It is shown that a particular concern, even in a facility with multiple acoustic enclosures, is the excitation of the lowest fundamental acoustic modes of the room by infrasound in the low tens of Hz range, and the efficient coupling of the fundamental room modes to a large inertia block centered in the room. *Published by AIP Publishing.* [http://dx.doi.org/10.1063/1.4962241]

## I. INTRODUCTION

In recent decades there have been revolutionary developments in measurement and fabrication tools that operate with spatial resolution on the atomic scale. These advances in spatial resolution bring with them a heightened sensitivity to unwanted vibrations on the same scale, requiring new strategies to minimize the impact of both mechanical and acoustic vibrations on a tool's performance. One of the most demanding of all such tools is the Scanning Tunneling Microscope (STM), which relies on precise positioning of a sharp metallic tip less than a nanometer from the surface of a sample. Achieving atomic resolution imaging of a surface by scanning the tip laterally above the surface clearly requires the horizontal position to be undisturbed by vibrations. More seriously, the STM measurement relies on the quantum-mechanical tunneling of electrons between the sample and tip and is exponentially sensitive to the tip-sample separation.[1] The exponential sensitivity is the source of both the technique's exquisite resolution and its extreme sensitivity to vibration.

Two tactics are commonly brought together to solve this problem. First, the STM head is designed to be compact and stiff, with resonant frequencies in the kHz range.[2] This makes the tunnel junction relatively insensitive to lower frequency vibrations, which move the tip and sample together in phase, without changing their separation.[3] This mitigation of the low-frequency noise is a particular advantage for STM techniques which rely on the measurement of a current on timescales of milliseconds to seconds. Second, the STM head is often suspended on springs, with the resonant frequency of the mass-spring system in the Hz range, followed by a $1/f^2$ roll-off at higher frequencies. This ensures that negligible ambient vibrations are transmitted to the STM head at the much higher frequencies where its resonances lie.[4] Some form of damping is generally added to the mass-spring system in order to reduce the amplification of ambient vibrations at its Hz-range resonant frequency.[4]

The entire system can be further isolated by supporting it on pneumatic vibration isolators, and a number of state-of-the-art STM facilities go even further by placing the system atop a massive inertia slab that is itself supported on large pneumatic isolators.[5,6] One or more layers of acoustic enclosure are also employed to prevent acoustic excitation of vibrations of the instrument. This more extreme approach is especially important for ultra-low-temperature STMs. In order to cool an STM head to sub-Kelvin temperatures, it must be firmly, mechanically attached to a cooling source such as the mixing chamber of a dilution fridge, and with substantial contact area. This precludes suspending the STM head on an internal damped spring system and means that all vibration isolation occurs outside the instrument.[5]

Isolation systems involving massive, floating slabs are employed in a wide range of applications and can be well-modelled at low frequencies as a damped mass-spring system, designed to have a resonant frequency near one Hz or lower. The measured performance typically exhibits nearly ideal 2nd-order transfer functions at low frequencies, but deviations in the form of excess vibration amplitude typically appear above 10-20 Hz.[5–10] There are many potential sources of such deviations, including rigid-body rolling modes of the slab, flexural modes, non-linearity in the response under test conditions, and acoustic excitation of the block motion. This latter source, referred to as acoustic buffeting or the sail-effect, is a known problem in a wide range of facilities ranging across fields such as metrology,[10] scanning electron microscopy,[11] medical imaging,[12] nanotechnology,[13] and the testing of components used in gravitational wave detection.[8,14] In many situations, acoustic noise sources such as ventilation systems are implicated, but acoustic buffeting has been discussed

a)Author to whom correspondence should be addressed. Electronic mail: bonn@phas.ubc.ca

even in the context of STM facilities where multiple acoustic enclosures are used, and ventilation is absent.[5] There is still a lack of consensus on how often acoustic buffeting is an issue in such facilities, and what are the best design practices. It is important to determine if this effect is relevant, since it may be a limitation in some existing facilities, and is presently driving differing approaches to the overall combination of acoustic and mechanical isolation employed. For instance, placing an inner acoustic enclosure on top of an inertia slab might be seen as a good way to shield the instrument inside from acoustic noise but might also enhance the acoustic driving of the slab itself. Here we show detailed measurements of our facility that provides an unambiguous demonstration that acoustic buffeting is a significant factor in the performance of a massive inertia block, even in the presence of substantial acoustic shielding. Measurements and modelling of this effect lead to several suggestions for the design of next-generation facilities.

## II. THE LOW VIBRATION FACILITY

The low vibration facility studied here is situated on a concrete foundation, separated from the foundation of the building and resting on compact glacial till. On top of this isolated foundation, an 80 tonne inertia block is supported by six pneumatic isolators. The isolators were manufactured by Integrated Dynamics Engineering (model IDE PD3001H) and are dual-chamber air-springs with an adjustable orifice for damping in the vertical direction. A low-temperature, ultra-high-vacuum STM apparatus is mounted on top of the inertia block. The experimental apparatus and inertia block are surrounded by a thick, double-walled acoustic enclosure. The inner walls of the enclosure are reinforced concrete anchored to the isolated foundation, while the outer walls are concrete block anchored to the building foundation. In order to damp the acoustic resonances bounded by hard concrete surfaces, acoustically absorptive material has been placed on nearly all of the surfaces in the space between the inner and outer acoustic enclosures, and also to any available space on the walls and ceiling of the inner vault. It is expected, however, that these acoustic treatments become increasingly ineffective below audible frequencies, and that infrasound in the enclosure can still be a significant issue. Access to the pods is through two sets of doors; the doors in the outer acoustic wall are solid core wood and rated STC-42, and those in the inner acoustic wall are steel and rated STC-59. A graphical overview of the design of the facility and inertia blocks is shown in Figure 1.

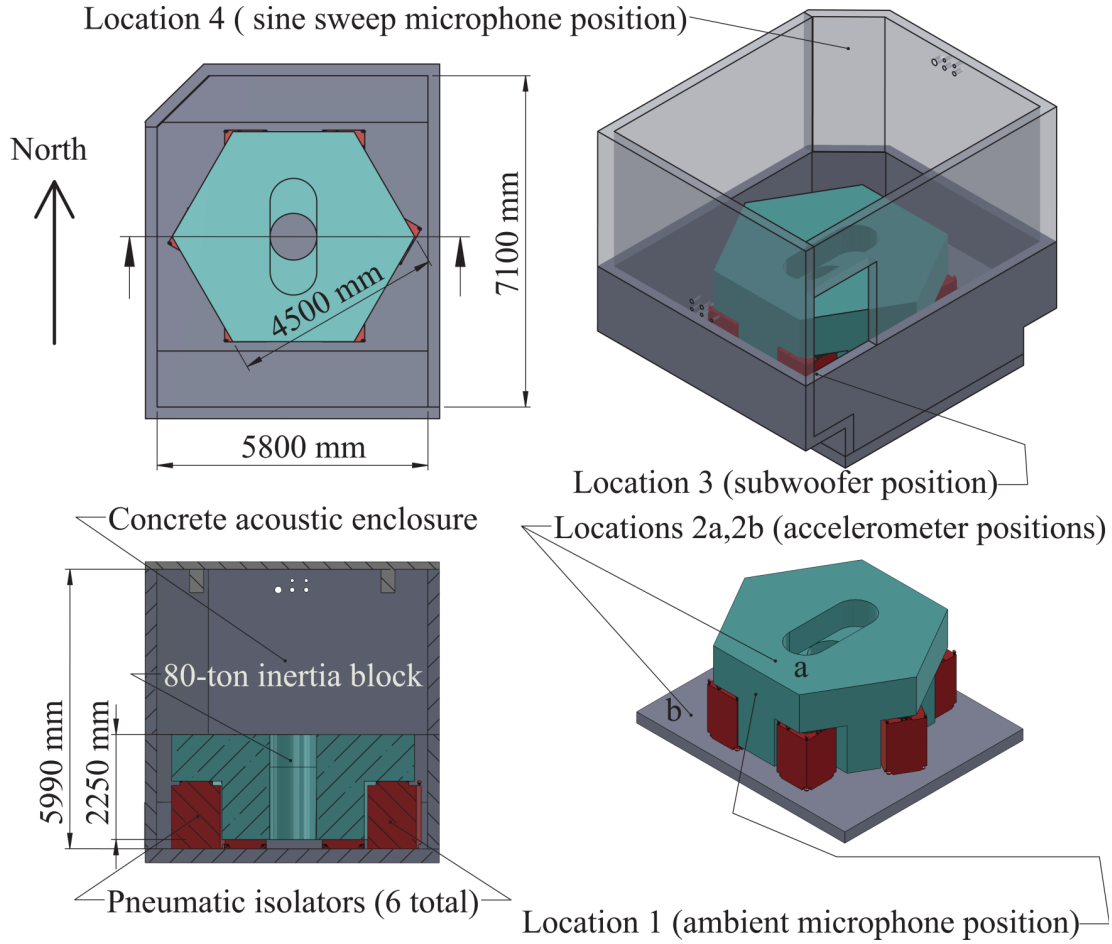


FIG. 1. Overview of the inertia block mounted on six pneumatic isolators. The inertia block, as well as the inner of two acoustic enclosures, sits on a foundation separate from the building. An outer acoustic enclosure sits on the building foundation. For the experiment, accelerometers were placed on the foundation and on the block (locations 2a, 2b), aligned to measure horizontal motion in the north-south direction. The ambient sound field was measured with a microphone beside the block (location 1). Ambient and driven sound measurements were also made in an upper corner of the room (location 4).

We consider two potential problems that may cause the inertia block's behavior to deviate from a simple damped mass-spring system. First, we consider rigid body rocking modes of the inertia block atop the isolators. For our system, the rocking modes have been measured to be in the 1-3 Hz regime so could contribute additional low-frequency resonant responses other than the single resonance of a simple 1-dimensional, mass-spring system. Second, the flexural modes of the slab were a particular consideration in the design shown here, with the design principle being to push the frequency of those flexural modes as high as possible, so that they are not excited by the ambient vibration spectrum, which is weighted towards low frequencies. A finite element optimization process was employed that resulted in a slab design that is relatively compact in all dimensions for the targeted mass of 80 tonnes. The hexagonal shape achieves very high frequencies for the lowest flexural resonant modes, and the as-built slab has its lowest measured flexural mode at 193 Hz.

The large frequency gap between the rigid body modes of the block-isolator system, and the block's lowest flexural mode, leaves a substantial range over which to look for effects outside those expected of a mass-spring system driven by only the mechanical vibrations of the underlying foundation.

## III. THE EXPERIMENT

To evaluate the performance of the inertia block, and to quantify the possible effects of acoustic buffeting, the block's horizontal acceleration spectrum, the foundation's horizontal acceleration spectrum, and the acoustic pressure were all measured simultaneously. The first measurements were performed under ambient vibration conditions, without artificial external drive, in order to best evaluate the block performance in real operating conditions.[15] We chose to measure horizontal, rather than vertical, accelerations because the pneumatic isolators have higher compliance and lower damping in the horizontal direction. Horizontal acoustic buffeting would also be of greater concern due to greater wall area in designs where the inner acoustic wall is placed atop the inertia block, rather than on the isolated foundation. Locations for the accelerometers and microphone are shown in Fig. 1. For consistency with existing literature, all measured linear acceleration spectral densities have been converted to linear velocity spectral densities by dividing by $i\omega$ at each angular frequency bin. Fig. 2(a) shows the foundation's horizontal velocity spectrum and the velocity spectrum for horizontal motion of the block. The foundation was measured with a PCB 393B04 accelerometer, and the inertia block was measured with a Wilcoxon 731A. The noise floors for each are also shown in Fig. 2(a). Acoustic measurements were made with Behringer ECM8000 omnidirectional electret condenser microphones powered by a Yorkville PGM8 mixer board. Both accelerometer and acoustic measurements were acquired through a PCI-4462 DAQ card. The spectra were acquired using 30 s long time series, sampled at 5 kHz, repeated and averaged over 30 h spanning a weekday and part of a weekend.

The ratio of block velocity divided by foundation velocity is shown in Fig. 2(b). If the block were simply a damped

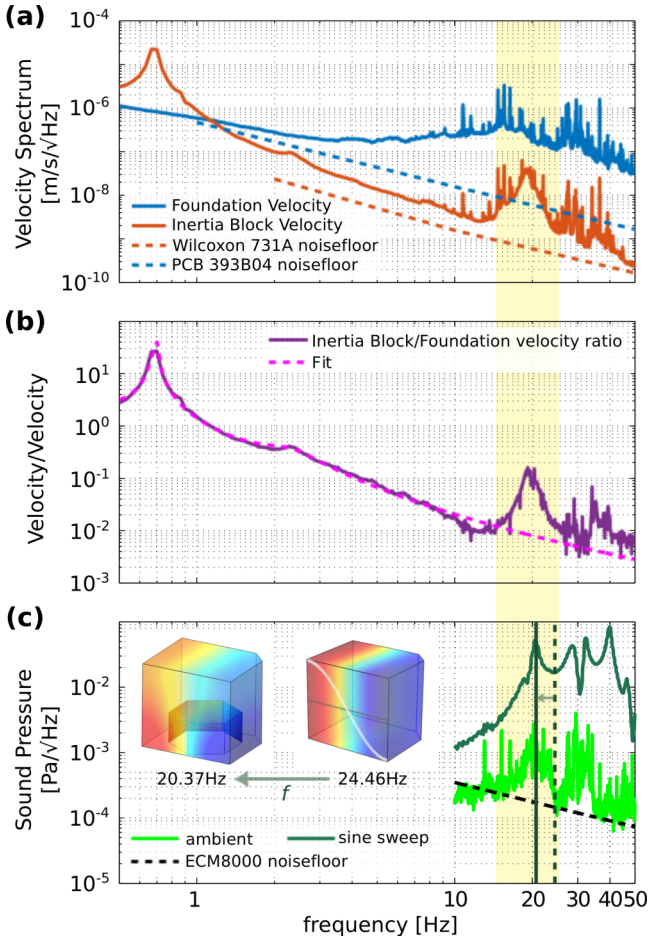


FIG. 2. (a) Foundation velocity spectrum (blue) and inertia block velocity (orange), for motion in the north-south direction. The spectra are acquired with 30 s time series, averaged over 30 h. Dashed lines indicate noise floors of the two sensors. (b) The ratio of the block velocity to the foundation velocity (purple). The dashed pink line is a fit to a transfer function that includes two rigid-body modes for the damped mass-spring system, the main peak at 0.67 Hz is the north-south resonant motion, and the weaker peak at 2.3 Hz is a rolling mode. An additional peak at 20 Hz is attributed here to acoustic buffeting. (c) The acoustic pressure spectrum was measured in an upper corner of the room (location 4 in Fig. 1) in order to capture sound modes in all directions. The ambient spectrum (light green curve) shows a peak at 20 Hz which appears to correspond to the excess velocity measured on the block. An FEA analysis of the room acoustics shows that the block shifts the lowest fundamental mode in the north-south direction from 24.46 Hz down to 20.37 Hz. The 20 Hz acoustic mode is further confirmed by measuring the room excited by a sub-woofer (dark green curve).

mass-spring system driven by the velocity spectrum of the foundation, this ratio should be an empirical measurement of that system's transfer function. However, here we consider a more general model that includes the possibility of a force $F$ acting directly on the inertia block. The equation of motion for a mass driven in both of these ways can be written as

$$m\ddot{x}_{mass} + b\dot{x}_{mass} + kx_{mass} = F + b\dot{x}_{base} + kx_{base}, \quad (1)$$

where $m$ is the mass of the inertia block, b is a linear damping parameter, and k a spring constant. $x_{mass}$ and its derivatives refer to the block motion, and $x_{base}$ and its derivatives refer to the motion of the foundation.

Below 10 Hz, the qualitative features are as expected. The main resonance at 0.69 Hz is in the range of expected

frequency for the fundamental rigid body mode (the block moving horizontally atop the isolators), and the shoulder at 2.3 Hz is in the right range for a rolling rigid body mode. If the force F in Eq. (1) is set to zero, one derives the transfer function relating the foundation velocity to the inertia block velocity, and the total vibrational transfer function is a sum over the two visible modes,

$$|H_{vibration}| = \frac{|V_{mass}|}{|V_{base}|} = \sum_{i=1}^{2} a_i \left[ \frac{1 + \left(2\zeta_i \frac{\omega}{\omega_{0i}}\right)^2}{\left(1 - \left(\frac{\omega}{\omega_{0i}}\right)^2\right)^2 + \left(2\zeta_i \frac{\omega}{\omega_{0i}}\right)^2} \right]^{\frac{1}{2}}, \quad (2)$$

where $\omega_{0i}$ are the resonant frequencies of the two modes, and $\zeta_i$ is a dimensionless damping parameter for each mode, with the quality factor of each mode being $Q = 1/(2\zeta_i)$, and the relative weights are $a_i$. A fit to this transfer function was made over the range 0.5-10.0 Hz and is shown as a dashed curve in Fig. 2(b). There are deviations in magnitude when this fit is extrapolated below 0.5 Hz, due to the foundation measurements approaching the noise floor of the PCB 393B04. A related, but opposite, deviation in overall magnitude occurs above 50 Hz due to the inertia block measurements approaching the noise floor of the Wilcoxon 731A.

The most striking deviation from the simple model is the prominent resonance near 20 Hz, too high in frequency to be a rigid-body rolling mode of the block, too low to be a flexural mode of the block, and not apparent as a feature in the foundation's velocity spectrum. Fig. 2(c), which shows a prominent feature at 20 Hz in the room's ambient acoustic spectrum (measured in the upper corner of the room, location 4 in Fig. 1), strongly suggests that the ambient acoustic noise is coupling to the block in this regime.

## IV. MODELLING THE ACOUSTIC FORCING OF AN INERTIA BLOCK

Since the block motion near 20 Hz looks very much like a resonant mode, it is natural to investigate the resonant modes of the inner acoustic enclosure. Acoustic energy in this infrasound regime is relatively difficult to block from entering the enclosure, and it is similarly challenging to strongly damp room acoustic resonances that might be excited by this leakage of infrasound into the room. Here, in our second set of measurements, we both model and measure the room's relevant acoustic modes, and then use this to further model the impact on the inertia block.

In addition to the ambient noise spectrum, Fig. 2(c) includes a measurement of driven acoustic resonant features in the room. Both were measured with a microphone placed in an upper corner of the room in order to best capture all room modes (location 4 in Fig. 1), but the driven resonances were measured by running a sub-woofer inside the enclosure (location 3 in Fig. 1), and then sweeping the drive frequency. The driven sound field exhibits a number of resonant features, the lowest being very close to the 20 Hz feature seen in both the room's ambient sound pressure and in the motion of the inertia block. Finite element analysis (FEA) treating the room as an empty box indicates that the lowest fundamental acoustic mode of the room is at 23 Hz. This is a mode in the long, north-south direction of the room, which is also the direction of motion measured on the inertia block. The room of course is not an empty box, and diffraction of acoustic waves around the block effectively increases the path length and lowers the fundamental resonant frequency (see Fig. 2(c) inset). When the block is included in the analysis, the lowest fundamental mode is shifted down to near 20 Hz, in good agreement with the lowest measured acoustic mode in the room. The particular importance of this lowest mode comes from two considerations. First, the ambient sound field in the room falls off at frequencies higher than the lowest fundamental acoustic modes, due to the better attenuation of the acoustic enclosures at shorter wavelengths. Above 60 Hz, the ambient sound spectrum is featureless and near the noise floor of the microphone. The second reason for the importance of the fundamental mode is that, in order to save space, inertia blocks typically extend close to the vertical inner surfaces of their acoustic enclosures. This enhances the coupling of the fundamental modes; the instantaneous forces add, since minimum pressure on one side of the room is reached (pulling on the block), just as maximum pressure is reached on the other side of the room (pushing on the block), as illustrated in Fig. 3. Finally, it is also worth highlighting the issue of mode orientation, as well as the phase issues that give rise to net forces on the block. Fig. 2(c) shows that there are also resonant modes and considerable ambient sound near 30 Hz, but FEA analysis shows that these are acoustic modes orthogonal to the block motion being measured here, so are not apparent as a resonance in the motion of the block in the north-south direction.

Following these considerations, we model the effect of the sound field on the motion of the inertia block, using a one-dimensional model for motion in the north-south direction. A simple 1-d analytical model of acoustic buffeting was

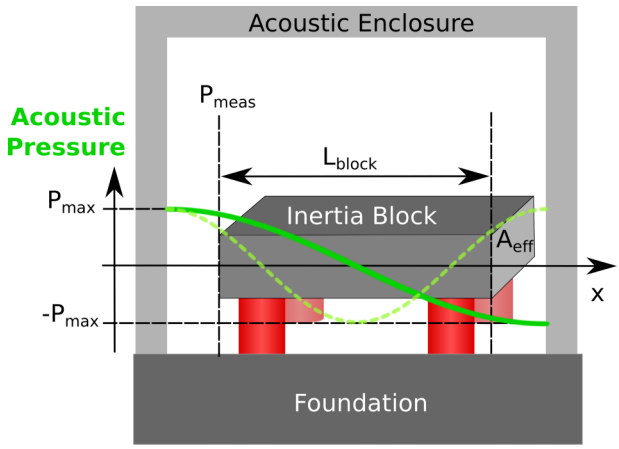


FIG. 3. A simplified, 1-dimensional model for treating the acoustic field coupling to the block at the low frequencies in the vicinity of the room's two lowest modes. The out-of-phase pressure antinodes of the fundamental mode (solid green) push and pull against an area $A_{eff}$, however, there is no net force caused by the next harmonic (dashed green).

previously proposed,[16] and here this model is modified by using the full second order force response transfer function, and by emphasizing the influence of the room modes. Consider a one-dimensional model of the force on a cuboidal inertia block, placed symmetrically within a room, as illustrated in Fig. 3. The block is driven by an acoustic standing wave, with pressure given by

$$P(x,t) = P_0 \times \cos\left(\frac{2\pi x}{\lambda}\right) \times \cos(2\pi f_n t) \tag{3}$$

with amplitude $P_0$, wavelength λ, and resonant frequency $f_n$. The pressure acts on a block with parallel opposing faces of equal area $A$. For the fundamental mode $f_1$, shown schematically with the green curve in Fig. 3, the inertia block has a pressure maximum on one face at the same time it has a pressure minimum on the opposite face. The net amplitude of the oscillating acoustic force on the block is $F_{Acoustic} = 2\ P_{meas}(f_1)\ A$, where $P_{meas}(f_1)$ is the measured sound pressure amplitude at the face of the block, at the room's lowest resonant frequency. In contrast, the net force exerted on the block at the next harmonic $f_2 = 2f_1$ is zero, as illustrated by the dashed green curve in Fig. 3. At frequencies off of these lowest resonances, travelling waves are still acting on the block, with sound pressures of order $P_{meas}(f)$, though typically rather less since the measured pressure is for waves travelling in all directions in the room, and the relative phases accounting for the net force on the block are unknown. A rough model for the frequency dependence of the force on the block that approximately takes into account both standing and travelling waves is

$$F_{Acoustic}(f) = P_{meas}(f) \times A \times \left(1 - \cos\left(\pi \frac{f}{f_0}\right)\right). \tag{4}$$

This model is similar to that employed by Fraumeni *et al.*,[16] who considered a block in free space, buffeted by travelling waves, where the resonance condition being considered was associated with half-wavelengths matching the block size. Here, in an enclosure, the term in parentheses in Eq. (4) instead emphasizes the resonance condition of the room. The value for A used was 8 $m^2$, an estimate based on the projected area of the hexagonal block, but reduced to account for the non-cuboidal shape. $P_{meas}(f)$ is the ambient acoustic spectrum measured with a microphone placed at the south face of the block (location 1 in Fig. 1). In order to include the effect of this driving force into the equation of motion for the block, one can derive a second transfer function from Eq. (1) by setting the base velocity to zero and considering the response to the acoustic force directly applied to the mass,

$$|H_{acoustic}| = \frac{|V_{mass}|}{|F_{acoustic}|} = \sum_{i=1}^{2} a_i \left[\frac{\frac{\omega^2}{\omega_{0i}{}^2 mk}}{\left(1 - \left(\frac{\omega}{\omega_{0i}}\right)^2\right)^2 + \left(2\zeta_i \frac{\omega}{\omega_{0i}}\right)^2}\right]^{\frac{1}{2}}. \tag{5}$$

The velocity of the inertia block in response to both the vibrations from the foundation and the acoustic driving force is then

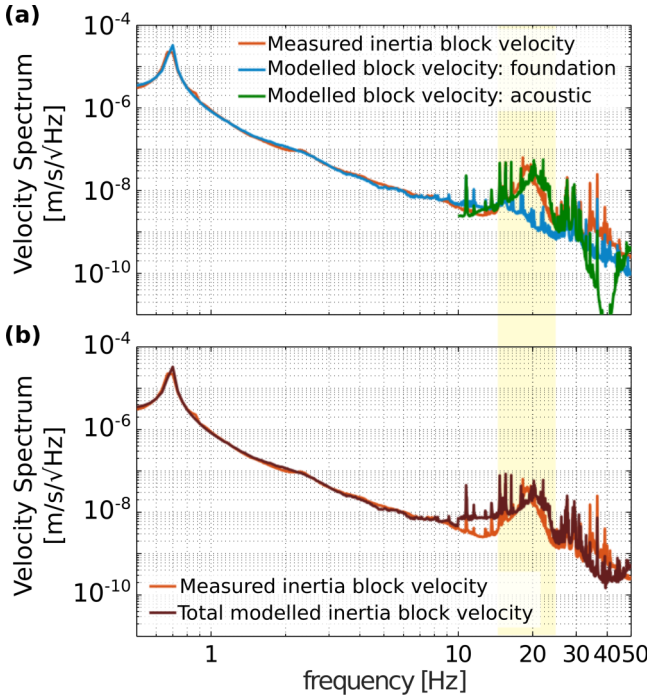


FIG. 4. (a) The measured inertia block velocity (orange) is compared to modeled contributions from foundation motion (blue) and acoustic buffeting calculated from the ambient acoustic spectrum measured on a block face (location 1) to best capture the force acting directly on the south face of the block (green). (b) The total modeled block velocity (brown) reproduces all of the main features in the data (orange) up to 50 Hz, with the acoustic buffeting being responsible for the prominent peak at 20 Hz.

$$V_{mass}(f) = V_{base}(f) \times H_{vibration}(f) + F_{acoustic}(f) \times H_{acoustic}(f). \tag{6}$$

Fig. 4 shows the results of this modelling of the inertia block motion. The blue curve in Fig. 4(a) shows the expected response of the block to the foundation motion, which closely matches the measured block motion from 0.5 to 10.0 Hz because that was the range used to determine the transfer function $H_{vibration}$. Above 10.0 Hz, this curve uses the extrapolation of that transfer function, multiplied by the measured foundation velocity, showing that there is no strong feature in the foundation velocity that is expected to come through the isolators and lead to a prominent feature near 20 Hz. The green curve in Fig. 4(a) corresponds to the block velocity predicted from the model for the acoustic buffeting, which does indicate that the measured sound field resonance near 20 Hz is capable of producing the degree of motion actually observed for the block in that range. The agreement between the measured and modelled effect is reasonable, despite the crude approximation of treating the inertia block as a cuboid, and the rough model for treating acoustic resonances and travelling waves. The sum of the acoustic and vibration terms shown in Fig. 4(b) does a good job of modeling the block motion from 0.5 to 50.0 Hz.

## V. CONCLUSIONS

This experiment on a particular vibration isolation facility demonstrates that acoustic buffeting can exert forces sufficient

to cause measurable motion of a massive inertia block, comparable in magnitude to transmitted floor vibrations. The prominent appearance of a fundamental acoustic mode of the room in the velocity spectrum of the inertia block highlights a particular set of conditions that can make this effect problematic. First, the lowest frequency, fundamental modes of the room will be the ones most excited by sound leakage into the room, simply due to the difficulty of attenuating such long wavelengths. Second, the fundamental horizontal modes will couple strongly to a block with faces close to opposite walls of the room, where the pressure is largest at the antinodes and has opposing phase that doubles the force on the block. Conversely, the second harmonic will generate little net force on such a block, and higher harmonics are likely to be attenuated by well-designed walls. Third, if the facility design involves a block with faces parallel to the pressure front (or isobaric surfaces) of such a mode, then the forces on the block can be relatively large since the pressure acts uniformly over the whole face. For the 20 Hz mode apparent here in the block motion, all three of these issues are present. Finally, for the specific application of low-temperature STM, the weak thermal links needed between the refrigerator stages can themselves have resonant pendulum-like modes in this frequency range, making it potentially sensitive to these frequencies, and even more important to tackle the acoustic buffeting problem at the lowest frequencies.

Our study carries a number of implications for the design of low-vibration facilities, and particularly highlights the importance of modeling and paying close attention to the coupling of an inertia block to the lowest-lying acoustic modes of a room. Ideally, the 3-dimensional shape and size of both the room and the block should be simulated more completely than the simple 1-dimensional model employed here. We suggest some general design features, in order to minimize acoustic buffeting. First, use extreme caution in implementing the common design that places an acoustic room on top of an inertia block, thereby greatly increasing its surface area without substantially increasing its inertial mass. Second, use larger air gaps between the block edges and the inner room walls, to separate the block edges from the extrema of the fundamental pressure wave. Third, consider alternative block and room geometries that avoid aligning the block surfaces with isobaric planes of the pressure antinodes of room modes. Finally, use tuned-damping to mitigate the most problematic room modes.

## ACKNOWLEDGMENTS

The authors acknowledge the contributions of Y. Pennec, G. Adamson, V. Wong, and A. Cote in the design and commissioning stages of the facility. C. Waltham and M. Hodgson provided advice and technical support with the measurements. This work was supported by The Natural Sciences and Engineering Research Council of Canada, Canada Excellence Research Chair program, the Canada Foundation for Innovation and BC Knowledge Development Fund, the Canadian Institute for Advanced Research, and the Stewart Blusson Quantum Matter Institute.

[1]G. Binnig, H. Rohrer, Ch. Gerber, and E. Weibel, Appl. Phys. Lett. **40**, 178 (1982).
[2]S. C. White, U. R. Singh, and P. Wahl, Rev. Sci. Instrum. **82**, 113708 (2011).
[3]C. R. Ast, M. Assig, A. Ast, and K. Kern, Rev. Sci. Instrum. **79**, 093704 (2008).
[4]M. Okano, K. Kajimura, S. Wakiyama, F. Sakai, W. Mizutani, and M. Ono, J. Vac. Sci. Technol., A **5**, 3313 (1987).
[5]Y. J. Song *et al.*, Rev. Sci. Instrum. **81**, 121101 (2010).
[6]S. Misra *et al.*, Rev. Sci. Instrum. **84**, 103903 (2013).
[7]K. Iwaya, R. Shimizu, T. Hashizume, and T. Hitosugi, Rev. Sci. Instrum. **82**, 083702 (2011).
[8]D. B. Newell *et al.*, Rev. Sci. Instrum. **68**, 3211 (1997).
[9]H. Amick, B. Sennewald, N. C. Pardue, C. Teague, and B. Scace, Noise Control Eng. J. **46**, 39 (1998).
[10]A. Lassila *et al.*, Measurement **44**, 399 (2011).
[11]D. A. Muller *et al.*, Ultramicroscopy **106**, 1033 (2006).
[12]W. R. Thornton, M. W. Trethewey, K. P. Maynard, and J. F. Sadler, Sound and Vibration **40**, 10 (2006).
[13]E. Lortscher, D. Widmer, and B. Gotsmann, Nanoscale **5**, 10542 (2013).
[14]J. Winterflood, Ph.D. thesis, University of Western Australia, 2001.
[15]F. B. Segerink, J. P. Korterik, and H. L. Offerhaus, Rev. Sci. Instrum. **82**, 065111 (2011).
[16]A. M. Fraumeni, P. Heiland, and N. Judell, Proc. SPIE **5933**, 59330T (2005).